ELSEVIER

Theoretical and Applied Fracture Mechanics 29 (1998) 67–74

theoretical and applied fracture mechanics

Influence of cracking on tensile behavior of brittle materials

A. Carpinteri *, F. Ciola

Politecnico di Torino, Department of Structural Engineering, 10129 Torino, Italy

Abstract

This paper deals with mechanical behavior of quasi-brittle materials in tension, such as concrete. Two elementary LEFM models are presented. Attention is focused on the crack phenomenon, highlighting the influence of initial damage on structural response. The first model consists of a plate of finite size with a central crack. The second model corresponds to an infinite plate with an infinite set of collinear cracks of equal length and spaced at a constant distance apart. For both models, an analytical study is conducted which leads to a determination of the link between critical stress and displacement, initially considering only the incremental displacement due to the damage present in the material, and subsequently also taking into account the elastic compliance of the structure. An analysis is also performed in which the concomitance of brittle fracture and plastic collapse is considered, which reveals interesting scale effects.

1. Introduction

In almost all engineering applications, the tensile strength of concrete is neglected during the design stage. In fact, the capacity of concrete to resist tension is not zero; it is often neglected because the tensile strength of concrete is considerably less than the compressive strength. Moreover, the tensile strength vary widely with the size of test specimen, aggregates, etc. The effects of these variables are difficult to account for. Concrete contains various types of inherent flaws, such as voids and microcracks, which have significant influence on the structural response. These defects cannot be disregarded in order to have a full understanding of the tensile behavior of concrete.

Typical experimental results of tensile tests can be described with reference to the load-displacement curve in Fig. 1. The linear portion is AB while strain hardening and softening correspond to BC and CD, respectively. The main point is to understand the role with which pre-existing flaws affect this behavior. Appropriate models need to be chosen to exhibit the tensile response of concrete.

2. Finite plate with central crack

2.1. Tensile mechanical behavior

To exhibit the tensile behavior of concrete, it is possible to use a cracked plate model as in Fig. 2. This configuration represents the structure damage at the initial stage. The stress–intensity factor for this problem is given by [1,2]

$$K_I = \sigma\sqrt{\pi a}\sqrt{\sec\left(\frac{\pi a}{2h}\right)}. \quad (1)$$

* Corresponding author. Tel.: +39 11 564 4850; fax: +39 11 564 4899; e-mail: carpinteri@polito.it.

0167-8442/98/$19.00
PII: S0167-8442(98)00017-2

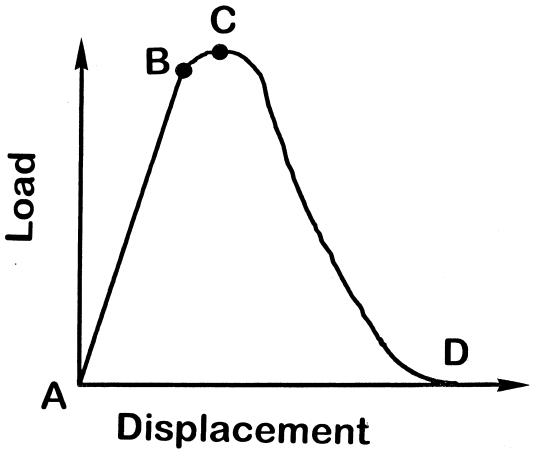

Fig. 1. Load-displacement diagram for concrete.

The displacement at infinity due to crack opening is

$$\delta = \frac{4\sigma a}{E} V2\left(\frac{a}{h}\right), \tag{2}$$

where

$$V2\left(\frac{a}{h}\right) = -1.071 + 0.250\left(\frac{a}{h}\right) - 0.357\left(\frac{a}{h}\right)^2 + 0.121\left(\frac{a}{h}\right)^3 - 0.047\left(\frac{a}{h}\right)^4 + 0.008\left(\frac{a}{h}\right)^5 - 1.071\frac{\ln\left(1-\left(\frac{a}{h}\right)\right)}{\left(\frac{a}{h}\right)}. \tag{3}$$

The relations given above apply in the case of a generic crack with an initial half-length of a_0. A linear relation between the displacement δ and the stress σ will be determined:

$$\delta = \frac{\sigma}{k}, \tag{4}$$

with

$$\frac{1}{k} = \frac{4h}{E}\frac{a_0}{h} V2\left(\frac{a_0}{h}\right). \tag{5}$$

The onset of crack motion is assumed to occur when $K_I = K_{IC}$. This leads to

$$\sigma_0\sqrt{\pi a_0}\sqrt{\sec\left(\frac{\pi a_0}{2h}\right)} = K_{IC}. \tag{6}$$

As Eq. (6) shows, the behavior of the material is strongly influenced by the geometry of the crack. The most significant factor is the ratio a_0/h, which may be regarded as the initial damage of the material ($a_0/h = 0$ with zero damage; $a_0/h = 1$ with complete separation).

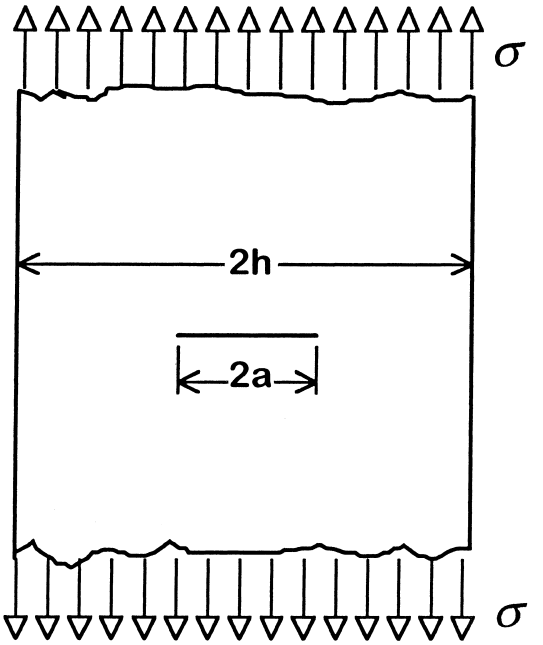

Fig. 2. Finite plate with central crack.

The incremental displacement is given by

$$\delta_0 = \frac{\sigma_0}{k} = \frac{K_{IC}}{\sqrt{\pi a_0}}\sqrt{\cos\left(\frac{\pi a_0}{2h}\right)}\frac{4h}{E}\frac{a_0}{h} V2\left(\frac{a_0}{h}\right). \tag{7}$$

when the crack has started to propagate, the behavior of the material may be obtained from Eqs. (1) and (2), by imposing the condition $K_I = K_{IC}$ for $a > a_0$. This gives

$$\sigma = \frac{K_{IC}}{\sqrt{\pi a}}\sqrt{\cos\left(\frac{\pi a}{2h}\right)}. \tag{8}$$

Recalling Eqs. (6) and (7), there results:

$$\frac{\sigma}{\sigma_0} = \sqrt{\frac{\cos\left(\frac{\pi a}{2h}\right)}{\cos\left(\frac{\pi a_0}{2h}\right)}}\frac{\sqrt{\frac{a_0}{h}}}{\sqrt{\frac{a}{h}}}, \tag{9}$$

$$\frac{\delta}{\delta_0} = \sqrt{\frac{\cos\left(\frac{\pi a}{2h}\right)}{\cos\left(\frac{\pi a_0}{2h}\right)}}\frac{\sqrt{\frac{a}{h}}}{\sqrt{\frac{a_0}{h}}}\frac{V2\left(\frac{a}{h}\right)}{V2\left(\frac{a_0}{h}\right)} \tag{10}$$

with $\frac{a_0}{h} \leqslant \frac{a}{h} \leqslant 1$.

Eqs. (9) and (10) are presented in graphical form in Fig. 3 for four different values of a_0/h

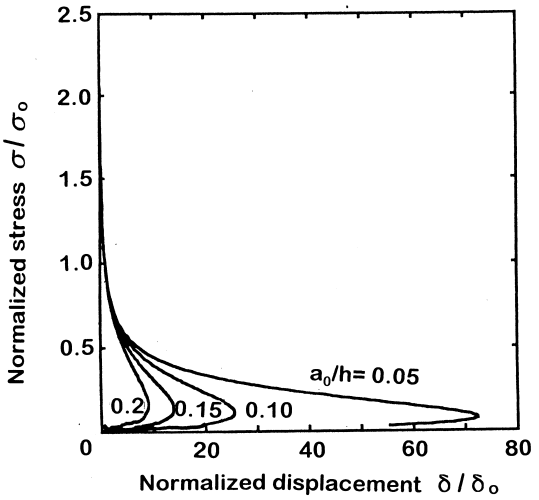

Fig. 3. Stress versus incremental displacement diagram.

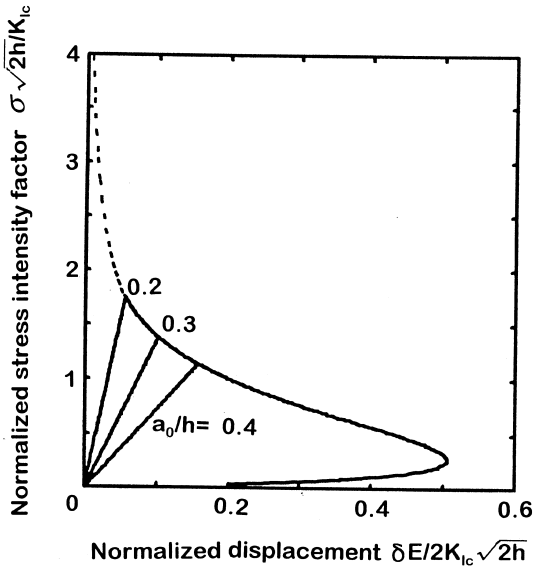

Fig. 4. Universal stress versus incremental displacement diagram.

$= 0.05$, 0.10, 0.15 and 0.20. The phenomenon of snap-back is noted in all cases. Initially, as a/h increases, the displacement also increases relative to the critical condition ($K_I = K_{IC}$), that is the increase in compliance prevails over the decrease in critical stress. Beyond a certain value of a/h, this displacement decreases. The value of a/h corresponding to this transition is indicated by a_c/h. It is determined by setting

$$\frac{\partial\left(\frac{\delta}{\delta_0}\right)}{\partial\left(\frac{a}{h}\right)} = 0. \tag{11}$$

This yields $a_c/h = 0.9288$. This value is independent of a_0/h. It can be used in Eqs. (8) and (2) to give the corresponding critical values σ_c and δ_c also being independent of a_0/h.

At first sight, this result would seem to be in disagreement with those obtained from Eqs. (9) and (10). However, Fig. 3 shows that as a_0/h grows, the ratio δ_c/δ_0 diminishes, and the ratio σ_c/σ_0 increases. Such an incongruence is only apparent and it is due to the variations of both δ_0 and σ_0 as a_0/h varies. Further elaboration on this will follow.

The linear portion ($K_I < K_{IC}$) as obtained from Eq. (2) gives

$$\delta = \frac{4\sigma h}{E}\frac{a_0}{h}V2\left(\frac{a_0}{h}\right). \tag{12}$$

For the softening branch, Eqs. (8) and (2) can be used to render:

$$\sigma = \frac{K_{IC}}{\sqrt{2h}}\sqrt{\frac{\cos\left(\frac{\pi a}{2h}\right)}{\frac{\pi a}{2h}}}, \tag{13}$$

$$\delta = \frac{4\sigma h}{E}\frac{a}{h}V2\left(\frac{a}{h}\right) \tag{14}$$

with $\frac{a_0}{h} \leqslant \frac{a}{h} \leqslant 1$.

Casting Eqs. (12)–(14) in dimensionless forms, and setting the nondimensionalized displacement on the abscissa and stress on the ordinate, it is possible to plot the $\sigma - \delta$ curve both in the linear portion and in the portion where softening occurs (Fig. 4). Note the point corresponding to the onset of the snap-back phenomenon. The softening branch, at its end portion, is common to all the cases considered. Initial cracking affects only the linear portion, beyond which the behavior of the material is uniquely determined by the condition of failure.

2.2. Virtual crack propagation

To evaluate the elastic deformation of the plate, consider a finite portion of length l. The displacement due to distributed elastic deformation is

$$\delta' = \frac{\sigma}{E} l. \tag{15}$$

The displacement due to the presence of the crack is expressed by Eq. (12) and shall be denoted by δ''. Superposition gives the total displacement as

$$\delta = \delta' + \delta''. \tag{16}$$

Using Eqs. (12) and (15) renders Eq. (16) dimensionless:

$$\frac{\delta E}{\sigma_P l} = \frac{\sigma}{\sigma_P}\left(1 + 4\frac{h}{l}\frac{a_0}{h} V2\left(\frac{a_0}{h}\right)\right). \tag{17}$$

Eq. (17) represents the nondimensionalized linear relation between load and displacement, which is found to be a function of both the initial relative crack length a_0/h and the ratio h/l. The term in brackets represents the nondimensionalized compliance. Fig. 5 shows some linear diagrams (for $h/l = 3$).

Recalling Eq. (6) and taking into account plastic collapse, it is possible to determine for each diagram both the point of brittle crack propagation and the point of plastic flow of the ligament. The former depends on the brittleness number [3,4], while the latter is unique. By joining the points that correspond to one and the same value of the brittleness number, a curve is obtained which represents the load-displacement link at the crack propagation. These curves are represented in Fig. 5, which also shows the curve joining the points of plastic collapse. From an analysis of the diagrams, there emerges a clear snap–back phenomenon due to the decrease in critical load and the increase in compliance.

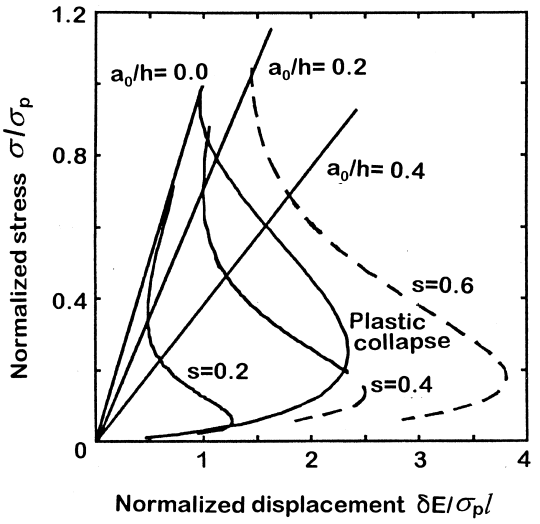

Fig. 5. Stress vs. displacement diagram for a finite portion of plate.

3. Infinite plate with ordered crack distribution

3.1. Tensile structural response

Another model for simulating the tensile mechanical behavior of concrete-like materials, is shown in Fig. 6. It consists of an infinite plate of unit thickness with an infinite set of collinear cracks of length $2a$ and located at a constant distance apart d. The stress intensity factor is [5]:

$$K_I = \sigma\sqrt{d\,\tan\left(\frac{\pi a}{d}\right)}. \tag{18}$$

The displacement at infinity due to the opening of the cracks is

$$\delta = \frac{4\sigma d}{\pi E}\ln\left(\sec\left(\frac{\pi a}{d}\right)\right). \tag{19}$$

The initial half-length of the cracks will be denoted by a_0. For this model, a linear relation is found between the displacement δ and the stress σ:

$$\delta = \frac{\sigma}{k}, \tag{20}$$

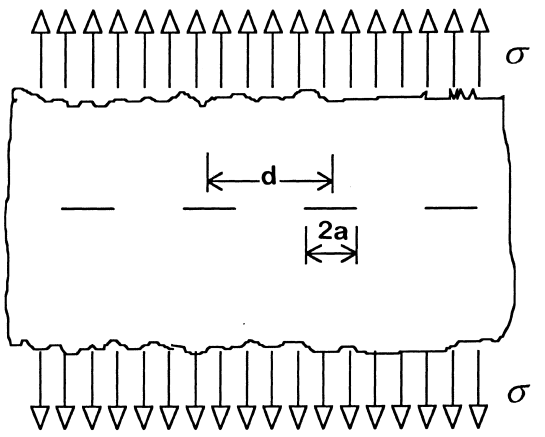

Fig. 6. Infinite plate with an ordered distribution of collinear cracks.

where

$$\frac{1}{k}=\frac{4d}{\pi E}\ln\left(\sec\left(\frac{\pi a_0}{d}\right)\right). \tag{21}$$

Crack propagation corresponds to $K_I = K_{IC}$. This leads to

$$\sigma_0\sqrt{d\,\tan\left(\frac{\pi a_0}{d}\right)}=K_{IC}. \tag{22}$$

The most significant factor is a_0/d, which may be considered as initial damage of the material ($a_0/d = 0$ with zero damage; $a_0/d = 0.5$ with complete separation). The incremental displacement is

$$\delta_0=\frac{\sigma_0}{k}=\frac{K_{IC}}{\sqrt{d\,\tan\left(\frac{\pi a_0}{d}\right)}}\frac{4d}{\pi E}\ln\left(\sec\left(\frac{\pi a_0}{d}\right)\right). \tag{23}$$

From Eqs. (18) and (19) for $K_I = K_{IC}$ and $a > a_0$, there results

$$\sigma=\frac{K_{IC}}{\sqrt{d\,\tan\left(\frac{\pi a}{d}\right)}}. \tag{24}$$

From Eqs. (22) and (23), it is found that:

$$\frac{\sigma}{\sigma_0}=\sqrt{\frac{\tan\left(\frac{\pi a_0}{d}\right)}{\tan\left(\frac{\pi a}{d}\right)}}, \tag{25}$$

$$\frac{\delta}{\delta_0}=\frac{\sigma}{\sigma_0}\frac{\ln\left(\sec\left(\frac{\pi a}{d}\right)\right)}{\ln\left(\sec\left(\frac{\pi a_0}{d}\right)\right)}. \tag{26}$$

Eqs. (25) and (26) are presented graphically in Fig. 7 for four different values of the initial crack depth $a_0/d = 0.010$, 0.015, 0.020, and 0.025; the snap–back phenomenon is noted in all cases. Initially, as a/d increases, the displacement corresponding to the critical condition ($K_I = K_{IC}$) also increases. That is the increase in compliance prevails over the decrease in critical stress. Beyond a certain value of a/d, the critical displacement decreases. The value of a/d that corresponds to this transition is indicated by a_c/d. It is determined by setting

$$\frac{\partial\left(\frac{\delta}{\delta_0}\right)}{\partial\left(\frac{a}{d}\right)}=0. \tag{27}$$

This gives $a_c/d = 0.4450$. Similar results are obtained in [6–9]. Note that the value found is independent of a_0/d. The same is applied to σ_c and δ_c.

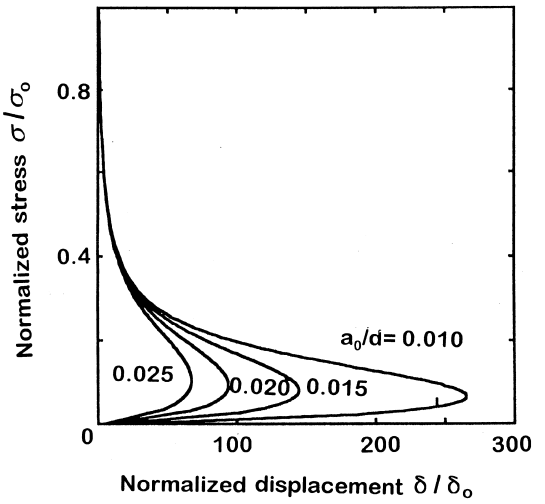

Fig. 7. Load vs. displacement relation during crack propagation.

For the linear portion ($K_I < K_{IC}$), the relation

$$\delta=\frac{4\sigma d}{\pi E}\ln\left(\sec\left(\frac{\pi a_0}{d}\right)\right) \tag{28}$$

prevails. Valid over are the relations:

$$\sigma=\frac{K_{IC}}{\sqrt{d\,\tan\left(\frac{\pi a}{d}\right)}}, \tag{29}$$

$$\delta=\frac{4\sigma d}{\pi E}\ln\left(\sec\left(\frac{\pi a}{d}\right)\right)=\frac{K_{IC}}{\sqrt{d\,\tan\left(\frac{\pi a}{d}\right)}}\frac{4d}{\pi E}\ln\left(\sec\left(\frac{\pi a}{d}\right)\right) \tag{30}$$

with $\frac{a_0}{d}\leqslant\frac{a}{d}\leqslant\frac{1}{2}$.

Recalling Eqs. (29) and (30) and setting the nondimensionalized displacement on the abscissa and nondimensionalized stress on the ordinate, it is possible to plot σ against δ both in the linear portion and in the portion where the softening phenomenon appears (Fig. 8). The snap–back initiation is found to be unique. Note that end portion of the softening branch, is common to all the cases considered. This is because the behavior of the material is related only to the condition of failure. Once the crack has reached a given length, its subsequent behavior is independent of its prior "history".

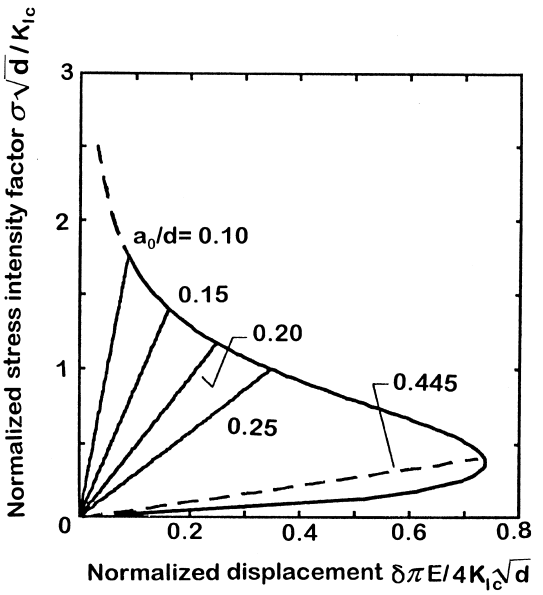

Fig. 8. Universal load vs. displacement relation during crack propagation.

The softening portion consists of two branches: one with a negative slope, in which the structural behavior could be detected by means of fixed-grip tests (deformation-controlled loading process), and one with a positive slope, in which the structural behavior could be detected by controlling the relative opening of the crack.

3.2. Evaluation of scale effects

Consider the model of Fig. 6. It is found from Eq. (19) that

$$\sigma_{\max} = \frac{K_{IC}}{\sqrt{d\,\tan\left(\frac{\pi a}{d}\right)}}, \tag{31}$$

which defines the load that causes crack propagation. Structural collapse could also occur by plastic flow of the ligament, i.e., of the material between two consecutive cracks. Although it never occurs for concrete, it is interesting to evaluate this behavior. Both types of collapse provide information for the scale effects.

Dividing Eq. (31) by the yield stress σ_P, the result is

$$\frac{\sigma_{\max}}{\sigma_P} = \frac{K_{IC}}{\sigma_P\sqrt{d}\sqrt{\tan\left(\frac{\pi a}{d}\right)}}. \tag{32}$$

Let us denote the *brittleness number* as follows:

$$s = \frac{K_{IC}}{\sigma_P\sqrt{d}}. \tag{33}$$

Eq. (32) becomes

$$\frac{\sigma_{\max}}{\sigma_P} = \frac{s}{\sqrt{\tan\left(\frac{\pi a}{d}\right)}}. \tag{34}$$

The plastic flow of the ligament under equilibrium requires that

$$\sigma_\infty d = \sigma_P(d - 2a), \tag{35}$$

where σ_∞ is the stress at infinity that causes the plastic flow of the ligament. Eq. (35) leads to

$$\frac{\sigma_\infty}{\sigma_P} = 1 - 2\frac{a}{d}. \tag{36}$$

To evaluate the scale effects, Eqs. (34) and (36) may be represented graphically as functions of a/d. The results are shown in Fig. 9. For low values of s, brittle propagation of the cracks precedes plastic flow of the ligament. The latter collapse phenomenon is always prevalent when a/d is close to zero (absence of crack) or is close to 1/2 (complete separation).

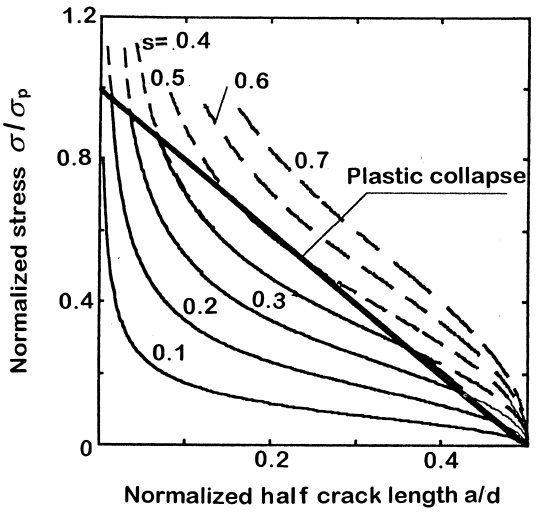

Fig. 9. Limit stress vs. relative crack length by varying the brittleness number.

For high values of s, plastic flow of the ligament precedes brittle propagation of the cracks. The value of s above which this situation occurs is approximately equal to 0.515. This behavior reflects what has already been highlighted for other geometries [10]. As the size scale increases, the behavior of the structure becomes brittle. This behavior does not depend on the individual quantities K_{IC}, d, and σ_P, but rather on their combinations.

3.3. Virtual propagation of cracks

The displacement due to the distributed elastic deformation is

$$\delta' = \frac{\sigma}{E} l, \tag{37}$$

where l represents the finite portion length. Displacement due to the presence of the crack is expressed by Eq. (19) and shall be denoted by δ''. By superposition, the total displacement is

$$\delta = \delta' + \delta''. \tag{38}$$

Put Eq. (38) in dimensionless form and consider Eqs. (19) and (37). It is found that

$$\frac{\delta E}{\sigma_P l} = \frac{\sigma}{\sigma_P}\left(1 + \frac{4}{\pi}\frac{d}{l}\ln\left(\sec\left(\frac{\pi a}{d}\right)\right)\right). \tag{39}$$

Eq. (39) represents the nondimensionalized linear relation between load and displacement, which is found to be a function both of the initial relative length of the crack a_0/d, and the ratio d/l. The term in brackets represents the nondimensionalized compliance. Fig. 10 presents some linear diagrams for $d/l = 1$.

From Eqs. (34) and (36), it is possible to determine the point of brittle propagation of the crack and the point of plastic flow of the ligament. The former depends on the brittleness number and the latter is unique.

For different values of a/d, the points for one and the same value of s which triggers crack propagation yield a curve that represents the load-displace relation for the phase of brittle collapse (Fig. 10).

A clear snap–back phenomenon may be noted because the decrease in critical load prevails over the increase in compliance. The thicker line represents the locus of the points characterized by plastic collapse on the residual section. In Fig. 10, as in Fig. 9, it may be noted that for low values of s, there is the intersection of the plastic collapse curve with the brittle fracture curve. For high values of s, the former type of collapse always prevails.

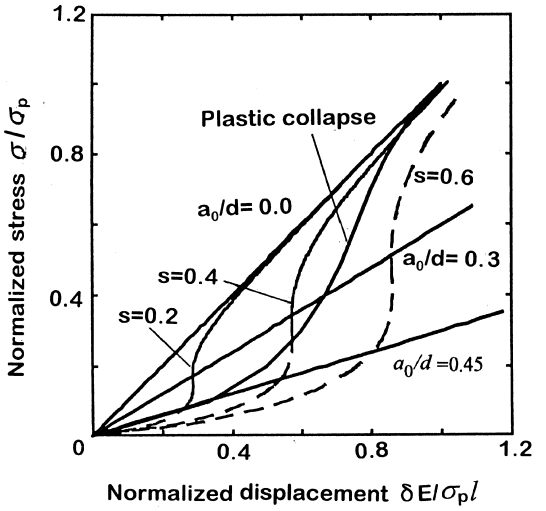

Fig. 10. Stress vs. displacement diagram for a finite portion of plate.

4. Conclusions

Crack propagation in brittle materials has been studied. The behavior of the two models qualitatively reflect experimental results. However, notable differences can appear at the end portion, that may be caused by the idealized geometries assumed.

It is also found that structural collapse does not depend exclusively on material strength, but it also depends on the material toughness and structural size. An explanation is thus provided for materials that are normally considered brittle and may behave in a ductile manner when test specimens of unusual small size are used (and vice versa).

Acknowledgements

The present research was carried out with the financial support of the Ministry of University and Scientific Research (MURST) and the National Research Council (CNR). Financial support from

the European Community TMR Contract n. ERBFMRXCT-960062, is also gratefully acknowledged.

References

[1] G.C. Sih, Handbook of Stress Intensity Factors, Institute of Fracture and Solid Mechanics, Lehigh University, Bethlehem, Pennsylvania, 1973.
[2] H. Tada, P.C. Paris, G.R. Irwin, The Stress Analysis of Cracks Handbook, Paris Productions Incorporated, St. Louis, Missouri, 1973.
[3] A. Carpinteri, Size effect in fracture toughness testing: A dimensional analysis approach, Proceedings of the International Conference on Analytical and Experimental Fracture Mechanics, 1980, 785–797.
[4] A. Carpinteri, Notch sensitivity in fracture testing of aggregative materials, Eng. Fract. Mech. 16 (1982) 467–481.
[5] Y. Murakami, Stress Intensity Factors Handbook, Pergamon Press, Oxford, 1987.
[6] H. Horii, A. Hasegawa, F. Nishino, Fracture process and bridging zone model and influencing factors in fracture of concrete, Proceedings of the SEM-RILEM International Conference on Fracture of Concrete and Rock, 1989, 205–219.
[7] M. Ortiz, Microcrack coalescence and macroscopic crack growth initiation in brittle solids, Int. J. Solids and Structure 24 (1988) 231–255.
[8] Z.P. Bazant, Stable states and stable paths of propagation of damage zones and interactive fracture, Proceedings of the France-US Workshop on Cracking and Damage, 1988, 183–200.
[9] B.L. Karihaloo, A. Carpinteri, M. Elices, Fracture mechanics of cement mortar and plain concrete, Advanced Cement Based Materials 1 (1993) 92–105.
[10] A. Carpinteri, Mechanical Damage and Crack Growth in Concrete, Martinus Nijhoff, Dordrecht, 1986.